

Theoretical investigation of temperature dependent elastic, thermophysical and ultrasonic properties of Sc-Ti-Zr-Hf quaternary alloy

Ramanshu Prabhakar Singh, Shakti Yadav, Devraj Singh, Giridhar Mishra
Veer Bahadur Singh Purvanchal University, Jaunpur, UP

Abstract

In this paper, we present computation of temperature dependent elastic, thermophysical and ultrasonic properties of HCP structured high entropy alloy Sc-Ti-Zr-Hf in the temperature range of 0-900K. By following the Lennard-Jones potential model, we have calculated second order elastic constants (SOECs) and third order elastic constants (TOECs) with the help of lattice parameters. SOECs and TOECs have been used to calculate the elastic parameters such as bulk modulus, shear modulus, Young's modulus and Poisson's ratio. With the help of SOECs, the ultrasonic velocities of different modes and Debye average velocity at different angle along unique axis have been computed. Further, with the help of Debye average velocity, the Debye temperature has been calculated, which, then, has been used to compute other thermal properties such as Debye heat capacity, thermal energy density and thermal conductivity at different temperatures. Additionally, we have estimated the ultrasonic attenuation due to different phenomena in solids which includes phonon-phonon interactions in different modes and thermoelastic relaxation mechanism in temperature range of 300-900K and found the attenuation due to the phonon-phonon interactions to be dominating over that due to thermo-elastic relaxation mechanism.

Keywords: hexagonal closed-packed, transition metal, quaternary alloy, refractory high entropy alloys

1. Introduction

In recent years, the high entropy alloys (HEAs) have become promising materials for advanced engineering applications[1-3]. This type of alloys contains more than four principal elements in near-equiatomic proportions. They are named 'high-entropy alloys' because the mixing entropies of their liquid or solid solutions states are significantly higher than that of conventional alloys[4-5]. Due to their distinct alloying arrangement, HEAs exhibit

many phenomenal properties such as high tensile strength, outstanding fracture toughness, and exceptional resistance to wear, tear, heat and corrosion[5-11]. These excellent properties of HEAs make them attractive in many fields with extreme temperature and pressure such as cryogenics[8-12]. Refractory elements such as Nb, Mo, Re, Ti, Zr, Hf etc. are well known for their excellent resistance to heat due to their high melting point[13-14]. Therefore, it is justified to assume that the high entropy alloys with refractory principal

*Corresponding Author(Email:ramanshupsingh@gmail.com)

elements *i.e.*, refractory high entropy alloys (RHEAs) will exhibit exceptional resistance to wear and tear, heat and corrosion at extreme temperature and pressure. In literature, most of the investigation on refractory metals and their alloys have been focused on body-centred-cubic (BCC) or face-centred-cubic (FCC)[1,6,7,10,15] with a very few closed-packed (HCP)[4,16-18] structured metal and metal alloys.

As elastic properties such as bulk modulus, shear modulus, Young's modulus and Poisson's ratio play important role in their consideration for engineering application and thermal properties like Debye temperature, heat capacity, thermal energy density and thermal conductivity help us understand their behaviour at different temperatures, it becomes important to study these alloys for these properties at different temperature.

Considering these exceptional properties of RHEAs, hexagonal closed-packed Sc-Ti-Zr-Hf becomes a promising RHEA to be extensively studied for enhancing and modifying mechanical, elastic and thermophysical properties of such materials.

Rai et al.[18] have theoretically estimated the mechanical, elastic and thermophysical properties of Sc-Ti-Zr-Hf at room temperature and other studies[19,20] experimentally determined its mechanical and thermal properties such as elastic moduli and thermal conductivity at variable temperature. Beside these studies, temperature dependence of third order elastic constants, thermal parameters such as Debye temperature, heat capacity, thermal energy density and ultrasonic velocities and attenuation of HCP Sc-Ti-Zr-Hf alloy are yet to be investigated. This motivates us to study these properties for Sc-Ti-Zr-Hf.

The present study produces the theoretical investigation of temperature dependent SOECs, TOECs, ultrasonic velocities of different modes along different direction, Debye average velocity, Debye temperature, heat capacity, thermal energy density, thermal conductivity and ultrasonic

attenuation due to different predominant phenomena for HCP Sc-Ti-Zr-Hf alloy.

2. Theory

For estimating the values of SOECs and TOECs at different temperature, we have utilized Brugger's definitions[21] of higher order elastic constants with the Lennard-Jones potential. The theoretical approach for estimating six independent SOECs and ten independent TOECs for HCP structured solids is meticulously described in the literature[22-26]. The different elastic moduli and related parameters have been estimated by Voigt-Reuss-Hill method[27,28] for hexagonal crystal solids. The longitudinal (V_L), quasi-shear (V_{S1}), shear (V_{S2}) ultrasonic velocities at different angles of propagation along unique axis (c-axis), Debye average velocity (V_D) and Debye temperature (θ_D) have been calculated utilizing the SOECs and TOECs by following the formulation discussed in literature[22,24-26,29].

Due to advanced engineering application of RHEAs in high temperature and pressures conditions, it becomes important to investigate their thermophysical behaviour at those extreme conditions. For computing the heat capacity (C_V) and thermal energy density (E_θ), we have used the Debye model for heat capacity[30-32].

The lattice thermal conductivity (κ) was evaluated by following the Morelli and Slack³³ approach which is given as:

$$\kappa = A \frac{M_a \theta_D^3 \delta}{\gamma^2 T n^{2/3}} \quad (1)$$

where A is a proportionality constant (with very slight dependence on Grüneisen number γ), M_a (in amu) is average atomic mass, θ_D is Debye temperature, δ is the cube root of volume per atom in Å, T is the temperature (in K), n is the number of atoms per unit cell and γ is Grüneisen number which can be determined by $\gamma = \frac{\alpha B}{C_V \rho}$ where α is the volume thermal expansion coefficient, B is bulk modulus, C_V is heat capacity and ρ is density of the material.

The ultrasonic attenuations in single crystal solids at high temperature are mostly due to phonon-phonon interactions (Akhiezer loss) and thermoelastic relaxation mechanism (thermoelastic loss). The formulation for estimating ultrasonic attenuation due to phonon-phonon interactions was developed by Mason and Bateman[34] and is given by:

$$\left(\frac{\alpha}{f^2}\right) = \frac{4\pi^2\tau_{th}E_0D}{2\rho V^3} \quad (2)$$

$$D = 9 \langle (\gamma_i^j)^2 \rangle - \frac{3\langle \gamma_i^j \rangle^2 C_V T}{E_0} \quad (3)$$

Where V is ultrasonic velocity in longitudinal and shear modes, $\langle (\gamma_i^j)^2 \rangle$ and $\langle \gamma_i^j \rangle^2$ are square average and average square Grüneisen numbers distinctive for longitudinal and shear modes and $\tau_{th} = \frac{3\kappa}{C_V V_D^2}$ is thermal relaxation time.

Thus, due to longitudinal and shear modes of ultrasonic waves, we have corresponding longitudinal $\left(\frac{\alpha}{f^2}\right)_L$ and shear $\left(\frac{\alpha}{f^2}\right)_S$ Akhiezer losses.

The ultrasonic attenuation due to thermoelastic relaxation mechanism were evaluated by:

$$\left(\frac{\alpha}{f^2}\right)_{th} = \frac{4\pi^2\langle \gamma_i^j \rangle^2 \kappa T}{2\rho V_L^5} \quad (4)$$

3.Results and Discussion

The SOECs and TOECs for Sc-Ti-Zr-Hf have been computed in the temperature range of 0-900K using lattice parameters available in literature[19] and presented in Fig. 1 and Fig. 2.

It is evident from Fig. 1 and 2 that SOECs decrease while TOECs increase or remain almost constant with increase in temperature. The SOECs also fulfil the mechanical stability criteria[23] for hexagonal structured crystal solids *i.e.*, $C_{44} > 0$, $C_{11} > |C_{12}|$, $(C_{11} + 2C_{12}) > 2C_{13}$. This confirms that the Sc-Ti-Zr-Hf alloy maintain

the mechanical stability over the temperature range 0-900K.

The evaluated values of bulk modulus (B), shear modulus (G) and Young's modulus (Y) are presented in Fig. 3. All of the elastic moduli *i.e.*, B , G , and Y decrease with increase in temperature but the Poisson's ratio is 0.2362 at 300K and remain almost constant throughout the temperature range 0-900K. The values of B , G , and Y at 300K are found to be 81.41GPa, 52.11GPa and 128.83GPa respectively which are in good agreement with the value available in literature[19,35].

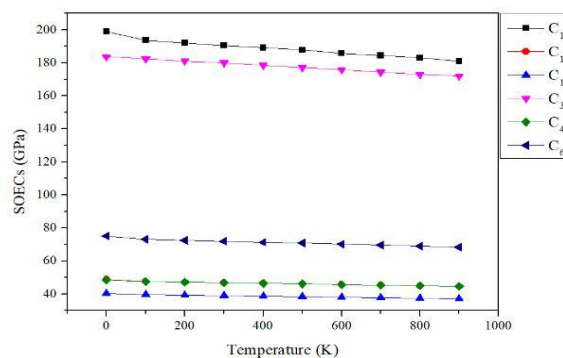


Fig. 1 – SOECs at different temperatures

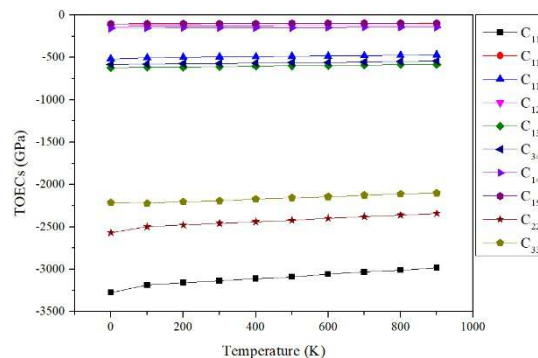


Fig. 2 – TOECs at different temperatures

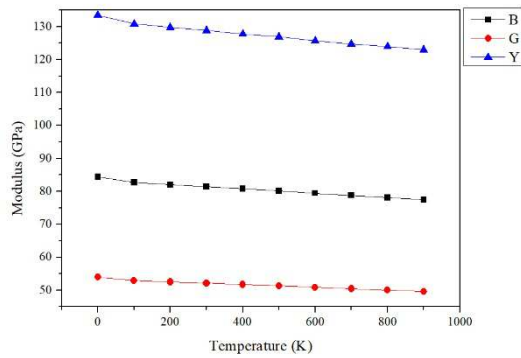


Fig. 3 – Temperature dependence of bulk modulus (B), shear modulus (G) and Young's modulus (Y)

The longitudinal (V_L), quasi-shear (V_{S1}) and shear (V_{S2}) and Debye average (V_D) ultrasonic velocities at different angles along the unique axis of HCP Sc-Ti-Zr-Hf crystal in the temperature range of 0-900 K were computed with the help of SOECs and density of the alloy from the literature[19] and presented in the Fig. 4.

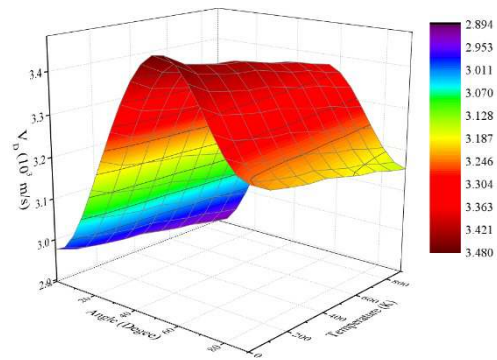
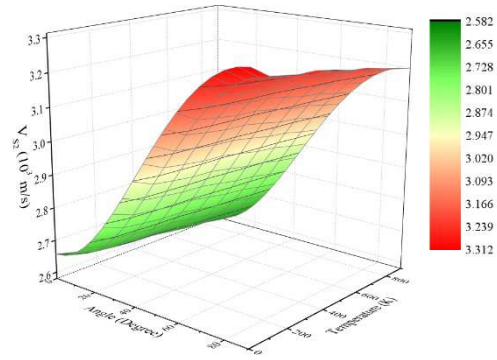
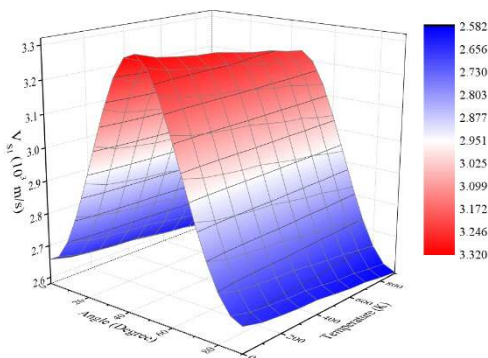
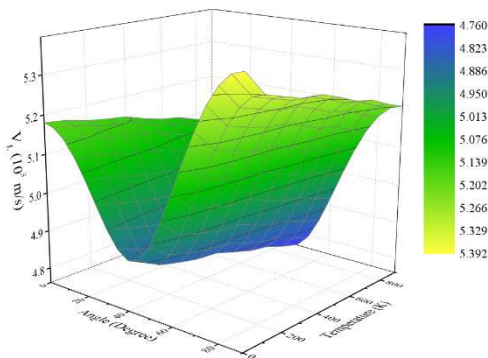


Fig. 4 – Longitudinal (V_L), quasi-shear (V_{S1}) and shear (V_{S2}) and Debye average (V_D) ultrasonic velocities at different temperatures.



The longitudinal ultrasonic velocity (V_L) decreases with increase in the angle θ from 0-45° with the unique axis but start increasing again from 45-90°. The quasi-shear ultrasonic velocity (V_{S1}) increases with increase in the angle θ from 0-45° but starts decreasing beyond 45°. The shear velocity (V_{S2}) monotonically increases with angle θ .

All of the longitudinal (V_L), quasi-shear (V_{S1}) and shear (V_{S2}) ultrasonic velocities decreases with increase in temperature. The maximum value of V_L has been found to be 5.39×10^3 m/s at angle 90° with the unique axis and 0K temperature. The Debye average velocity (V_D) follows trend similar to quasi-shear velocity (V_{S1}) with maximum value of 3.48×10^3 m/s at angle $\theta=55^\circ$ with unique axis and 0K temperature. The temperature dependence of ultrasonic velocities for HCP Sc-Ti-Zr-Hf have not been found in literature but is in good agreement with the values of these velocities at room

temperature[18] and of similar materials[25,36].

The Debye temperature (θ_D) is 311.66K at 300K and decreases from 316.08K to 305.00K in temperature range of 0-900K.

The computed values of heat capacity (C_V) and thermal energy density (E_θ) at different temperature in range of 0-900K are plotted in Fig. 5.

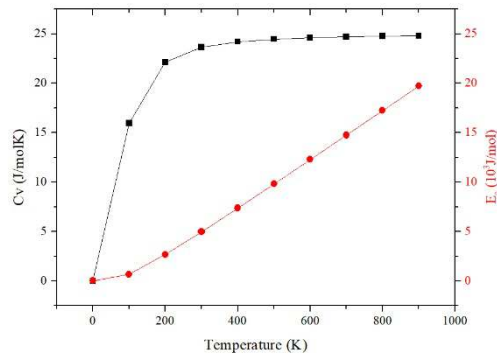


Fig. 5 – Temperature dependence of heat capacity (C_V) and thermal energy density (E_θ)

From Fig. 5, it is clear that C_V increases with temperature but increment becomes less and less as the temperature increases making the plot plateau at higher temperature. The thermal energy density (E_θ) increases with increase in temperature and shows an almost constant slope with temperature.

The thermal conductivity is one of the important thermal properties of a material and to compute it we used Eq. (1). The temperature and direction dependence of thermal conductivity (κ) is presented in Fig. 6.

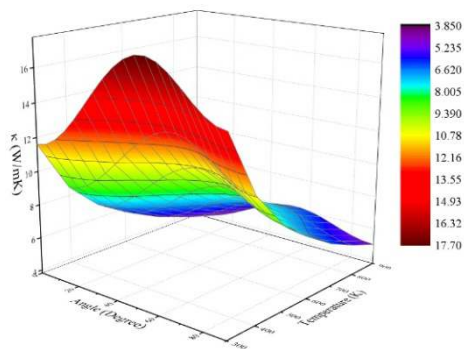


Fig. 6 – Temperature and direction (angle, θ) dependence of thermal conductivity (κ)

The thermal conductivity (κ) is found to be 11.60 W/mK at 300K and 0° angle with unique axis and decreases with increase in temperature and increases with increase in angle. The temperature dependence of thermal conductivity (κ) along unique axis is plotted in Fig. 7.

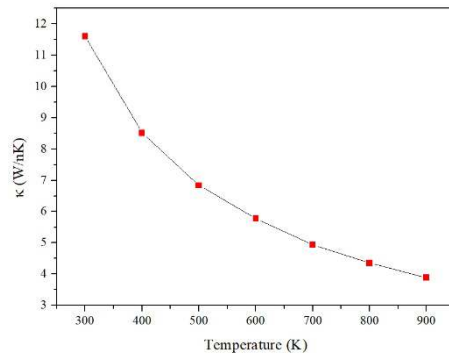


Fig. 7 – Temperature dependence of thermal conductivity (κ) along unique axis ($\theta=0^\circ$)

The alloy is not magnetically ordered, therefore, thermal conductivity is the sum of the electron and phonon contributions only[20]. On comparing thermal conductivity, which is only due to phonon contribution, at different temperature along unique axis in present study with thermal conductivity at those temperatures experimentally estimated in literature[20], we find that the experimental values follow opposite trend to that of in present study. This can be justified by the fact that the electronic thermal conductivity dominates at higher temperatures and lattice thermal conductivity (due to phonons) decreases with temperature[37].

Further, as the ultrasonic attenuation is directly correlated to thermoelastic properties and nature of bonds in a material, the ultrasonic attenuation due to phonon-phonon interaction (Akhiezer loss) and due to thermoelastic relaxation mechanism have been evaluated in temperature range of 300-900K and presented in Fig. 8.

The longitudinal ultrasonic attenuation (α/f^2)_L has a maximum value of 388.11×10^{-17} Np s²/m at temperature 900K and angle (θ) 45° and a minimum value of 182.38×10^{-17} Np s²/m at 300K of

temperature and 90° angle (θ) with unique axis. Akhiezer[38] have suggested that the attenuation due phonon-phonon interaction dominates over other form of attenuation at high temperature and the plots in Fig. 8 confirms this. The thermoelastic attenuation (α/f^2) is in range of $6.07 \times 10^{-24} - 13.98 \times 10^{-24} \text{ Nps}^2/\text{m}$ in temperature range of 300-900K.

The total ultrasonic attenuation (α/f^2)_{Total} is the sum of ultrasonic attenuation due to phonon-phonon interactions (both longitudinal and shear modes) and thermoelastic attenuation and is also presented in Fig. 8.

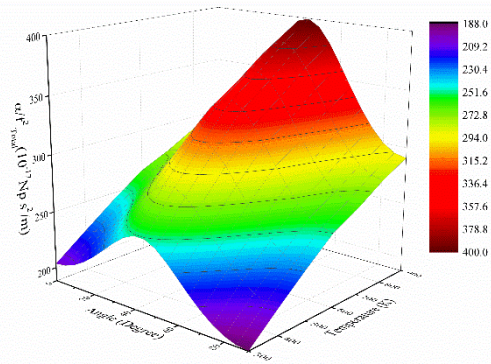
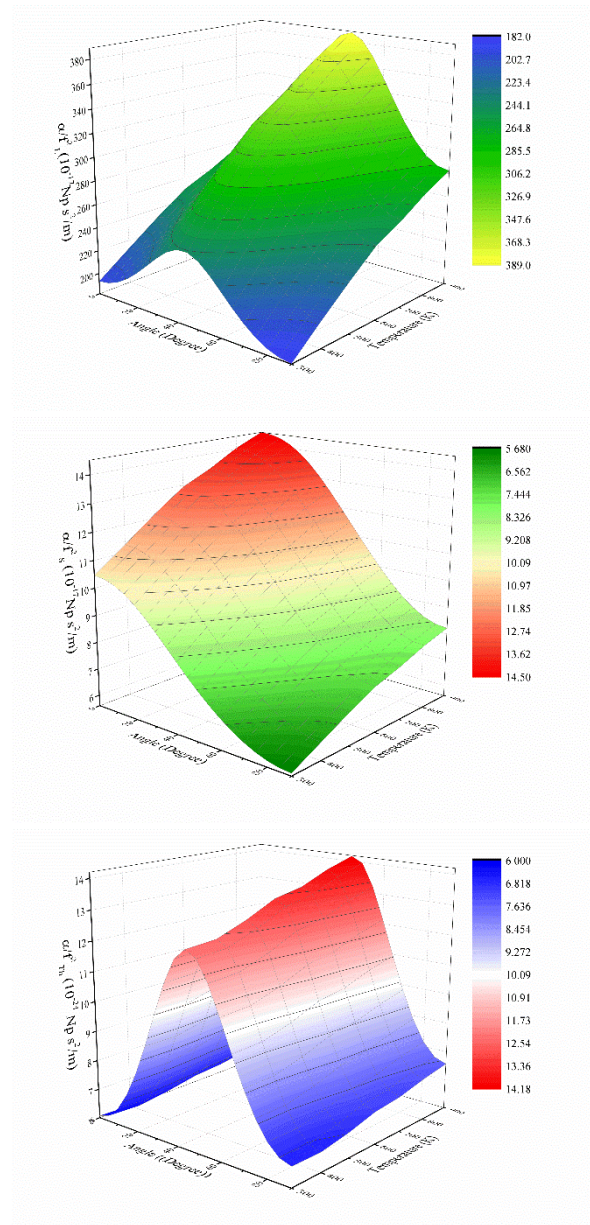


Fig. 8 – Direction and temperature dependence of longitudinal α/f^2 , shear α/f^2 , thermoelastic α/f^2 and total α/f^2 ultrasonic attenuation



4. Conclusion

On the basis of above results and discussion, the following conclusions have been drawn:

- The obtained results are in good agreements with other investigations available in literature. This demonstrates successful application of theoretical approach of ultrasonic non-destructive testing to determine elastic and thermophysical properties of solid materials.
- The RHEA alloy Sc-Ti-Zr-Hf shows strong mechanical stability in temperature range 0-900K.
- The heat capacity follows Dulong-Petit law.
- The thermal conductivity varies from 11.60 W/mK to 3.88 W/mK with varying temperature from 300K to 900K.
- The longitudinal ultrasonic attenuation is predominant over other forms of ultrasonic attenuation.

References

- Yeh J W, Chen S K, Lin S J, Gan J Y, Chin T S, Shun T T, Tsau C H & Chang S Y., Nanostructured High-Entropy Alloys with Multiple Principal Elements: Novel Alloy Design Concepts and Outcomes, Adv. Eng. Mater.6, 299–303 (2004) <https://doi.org/10.1002/adem.200300567>.
- Cantor B, Chang I T H, Knight P & Vincent A J B., Microstructural development in equiatomic multicomponent alloys, Mater. Sci.

- Eng. **A375–377**, 213–218 (2004)
<https://doi.org/10.1016/j.msea.2003.10.257>.
- [3] George E P, Raabe D & Ritchie R O., High-entropy alloys, *Nat. Rev. Mater.***4**, 515–534 (2019) <https://doi.org/10.1038/s41578-019-0121-4>.
- [4] Tsai M-H & Yeh J-W., High-Entropy Alloys: A Critical Review, *Mater. Res. Lett.***2**, 107–123 (2014)
<https://doi.org/10.1080/21663831.2014.912690>.
- [5] Hsu Y-J, Chiang W-C & Wu J-K., Corrosion behavior of FeCoNiCrCux high-entropy alloys in 3.5% sodium chloride solution, *Mater. Chem. Phys.***92**, 112–117 (2005)
<https://doi.org/10.1016/j.matchemphys.2005.01.001>.
- [6] Li D, Li C, Feng T, Zhang Y, Sha G, Lewandowski J J, Liaw P K & Zhang Y., High-entropy Al_{0.3}CoCrFeNi alloy fibers with high tensile strength and ductility at ambient and cryogenic temperatures, *Acta Mater.***123**, 285–294 (2017)
<https://doi.org/10.1016/j.actamat.2016.10.038>.
- [7] Yao M J, Pradeep K G, Tasan C C & Raabe D., A novel, single phase, non-equiatomic FeMnNiCoCr high-entropy alloy with exceptional phase stability and tensile ductility, *Scr. Mater.***72–73**, 5–8 (2014)
<https://doi.org/10.1016/j.scriptamat.2013.09.030>.
- [8] Gludovatz B, Hohenwarter A, Catoor D, Chang E H, George E P & Ritchie R O., A fracture-resistant high-entropy alloy for cryogenic applications, *Science (80-.)***345**, 1153–1158 (2014)
<https://doi.org/10.1126/science.1254581>.
- [9] Zhang Y, Zuo T T, Tang Z, Gao M C, Dahmen K A, Liaw P K & Lu Z P., Microstructures and properties of high-entropy alloys, *Prog. Mater. Sci.***61**, 1–93 (2014)
<https://doi.org/10.1016/j.pmatsci.2013.10.001>.
- [10] Hemphill M A, Yuan T, Wang G Y, Yeh J W, Tsai C W, Chuang A & Liaw P K., Fatigue behavior of Al_{0.5}CoCrCuFeNi high entropy alloys, *Acta Mater.***60**, 5723–5734 (2012)
<https://doi.org/10.1016/j.actamat.2012.06.046>.
- [11] Gorr B, Azim M, Christ H-J, Mueller T, Schliephake D & Heilmaier M., Phase equilibria, microstructure, and high temperature oxidation resistance of novel refractory high-entropy alloys, *J. Alloys Compd.***624**, 270–278 (2015)
<https://doi.org/10.1016/j.jallcom.2014.11.012>.
- [12] Hebda J., Niobium alloys and high temperature applications, in *Niobium, Science and Technology* 243–259 (2001).
- [13] Srikanth M, Annamalai A R, Muthuchamy A & Jen C-P., A Review of the Latest Developments in the Field of Refractory High-Entropy Alloys, *Crystals***11**, 612 (2021)
<https://doi.org/10.3390/cryst11060612>.
- [14] Duan J-M, Shao L, Fan T-W, Chen X-T & Tang B-Y., Intrinsic mechanical properties of hexagonal multiple principal element alloy TiZrHf: An ab initio prediction, *Int. J. Refract. Met. Hard Mater.***100**, 105626 (2021)
<https://doi.org/10.1016/j.jrmhm.2021.105626>.
- [15] Li R-X, Qiao J-W, Liaw P K & Zhang Y., Preternatural Hexagonal High-Entropy Alloys: A Review, *Acta Metall. Sin. (English Lett.)***33**, 1033–1045 (2020)
<https://doi.org/10.1007/s40195-020-01045-9>.
- [16] Huang T, Jiang H, Lu Y, Wang T & Li T., Effect of Sc and Y addition on the microstructure and properties of HCP-structured high-entropy alloys, *Appl. Phys.***A125**, 180 (2019)
<https://doi.org/10.1007/s00339-019-2484-1>.
- [17] Rogal L, Bobrowski P, Körmann F, Divinski S, Stein F & Grabowski B., Computationally-driven engineering of sublattice ordering in a hexagonal AlHfScTiZr high entropy alloy, *Sci. Rep.***7**, 2209 (2017)
<https://doi.org/10.1038/s41598-017-02385-w>.
- [18] Rai S, Chaurasiya N & Yadava P K., Elastic, Mechanical and Thermophysical properties of Single-Phase Quaternary ScTiZrHf High-Entropy Alloy, *Phys. Chem. Solid State***22**, 687–696 (2021)
<https://doi.org/10.15330/pcss.22.4.687-696>.
- [19] Huang S, Cheng J, Liu L, Li W, Jin H & Vitos L., Thermo-elastic behavior of hexagonal Sc–Ti–Zr–Hf high-entropy alloys, *J. Phys. D: Appl. Phys.***55**, 235302 (2022)
<https://doi.org/10.1088/1361-6463/ac50ce>.
- [20] Uporov S, Estemirova S K, Bykov V A, Zamyatin D A & Ryltsev R E., A single-phase ScTiZrHf high-entropy alloy with thermally stable hexagonal close-packed structure, *Intermetallics***122**, 106802 (2020)
<https://doi.org/10.1016/j.intermet.2020.106802>.
- [21] Brugger K., Thermodynamic Definition of Higher Order Elastic Coefficients, *Phys. Rev.***133**, A1611–A1612 (1964)
<https://doi.org/10.1103/physrev.133.a1611>.
- [22] Singh S P, Singh G, Verma A K, Jaiswal A K & Yadav R R., Mechanical, Thermophysical, and Ultrasonic Properties of Thermoelectric HfX₂ (X = S, Se) Compounds, *Met. Mater. Int.***2**, 1–9 (2020)
<https://doi.org/10.1007/s12540-020-00633-9>.
- [23] Nye J F., *Physical Properties of Crystals: Their Representation by Tensors and Matrices*, (Oxford University Press, 1985).
- [24] Jyoti B, Singh S P, Gupta M, Tripathi S, Singh D & Yadav R R., Investigation of zirconium nanowire by elastic, thermal and ultrasonic analysis, *Zeitschrift für Naturforsch.* **A75**,

- 1077–1084 (2020) <https://doi.org/10.1515/zna-2020-0167>.
- [25] Singh R P, Yadav S, Mishra G & Singh D,. Pressure dependent ultrasonic properties of hcp hafnium metal, *Zeitschrift fur Naturforsch. - Sect. A J. Phys. Sci.***76**, 549–557 (2021) <https://doi.org/10.1515/zna-2021-0013>.
- [26] Yadawa P K, Pandey D K, Singh D, Yadav R R & Mishra G,. Computations of ultrasonic parameters of lanthanide metals Ti, Zr and Hf, *Turkish J. Phys.***34**, 23–31 (2010) <https://doi.org/10.3906/fiz-0902-7>.
- [27] Saidi F, Benabadiji M K, Faraoun H I & Aourag H,. Structural and mechanical properties of Laves phases YCu₂ and YZn₂: First principles calculation analyzed with data mining approach, *Comput. Mater. Sci.***89**, 176–181 (2014) <https://doi.org/10.1016/j.commatsci.2014.03.053>.
- [28] Hill R,. Elastic properties of reinforced solids: Some theoretical principles, *J. Mech. Phys. Solids***11**, 357–372 (1963) [https://doi.org/10.1016/0022-5096\(63\)90036-x](https://doi.org/10.1016/0022-5096(63)90036-x).
- [29] Tripathi S, Agarwal R & Singh D,. Elastic, Mechanical and Ultrasonic Properties of Nanostructured IIIrd Group Phosphides, *MAPAN* (2020) doi:10.1007/s12647-020-00412-2 <https://doi.org/10.1007/s12647-020-00412-2>.
- [30] Singh S P, Singh G, Verma A K, Yadawa P K & Yadav R R,. Ultrasonic wave propagation in thermoelectric ZrX₂(X=S,Se) compounds, *Pramana - J. Phys.***93**, 83 (2019) <https://doi.org/10.1007/s12043-019-1846-8>.
- [31] Debye P,. Zur Theorie der spezifischen Wärmen, *Ann. Phys.***344**, 789–839 (1912) <https://doi.org/10.1002/andp.19123441404>.
- [32] Kittel C,. *Introduction to Solid State Physics*, (John Wiley & Sons, Inc, 2005).
- [33] Morelli D T & Slack G A,. High Lattice Thermal Conductivity Solids, in *High Thermal Conductivity Materials* (eds. Shindé, S. . L. & Goela, J. S.) 37–68 (Springer-Verlag, 2006). doi:10.1007/0-387-25100-6_2 https://doi.org/10.1007/0-387-25100-6_2.
- [34] Mason W P & Bateman T B,. *Ultrasonic-Wave Propagation in Pure Silicon and Germanium*, *J. Acoust. Soc. Am.***36**, 644–652 (1964) <https://doi.org/10.1121/1.1919031>.
- [35] Rogal Ł, Czerwinski F, Jochym P T & Litynska-Dobrzynska L,. Microstructure and mechanical properties of the novel Hf₂₅Sc₂₅Ti₂₅Zr₂₅ equiatomic alloy with hexagonal solid solutions, *Mater. Des.***92**, 8–17 (2016) <https://doi.org/10.1016/j.matdes.2015.11.104>.
- [36] Singh D, Mishra G, Kumar R & Yadav R R,. Temperature Dependence of Elastic and Ultrasonic Properties of Sodium Borohydride, *Commun. Phys.***27**, 151 (2017) <https://doi.org/10.15625/0868-3166/27/2/9615>.
- [37] Ho C Y, Ackerman M W, Wu K Y, Oh S G & Havill T N,. Thermal conductivity of ten selected binary alloy systems, *J. Phys. Chem. Ref. Data***7**, 959–1178 (1978) <https://doi.org/10.1063/1.555583>.
- [38] Akhiezer A,. On the Absorption of Sound in Solids, *J. Phys.***1**, 277–287 (1939).